

Neurotoxicity to dopamine neurons after the serial exposure to alcohol and methamphetamine: Protection by COX-2 antagonism

Amanda L. Blaker^{a,1}, Eric A. Rodriguez^{b,1}, Bryan K. Yamamoto^{b,*}

^a University of Toledo College of Medicine, Department of Neurosciences, 3000 Arlington Avenue, Toledo, OH 43614, USA

^b Indiana University School of Medicine, Department of Pharmacology & Toxicology, 635 Barnhill Drive, Indianapolis, IN 46202, USA

ABSTRACT

A significant co-morbidity exists between alcohol and methamphetamine (Meth) in humans but the consequences and mechanisms underlying their co-morbid effects remain to be identified. A consequence associated with the abuse of either alcohol or Meth involves inflammation but little is known about the role of inflammation in a possible neurotoxicity arising from their co-exposure. Sprague Dawley rats were allowed 28 days of intermittent, voluntary access to 10% ethanol (EtOH) followed by a neurotoxic binge administration of Meth. EtOH drinking followed by Meth increased microglial cell counts and produced morphological changes in microglia of the substantia nigra pars compacta 2 h after Meth administration that were distinct from those produced by either EtOH or Meth alone. These effects preceded the activation of cleaved caspase-3 in dopamine cell bodies, as well as decreases in tyrosine hydroxylase (TH) immunoreactivity in the substantia nigra and dopamine transporter (DAT) immunoreactivity in the striatum measured at 7 days after Meth. Intervention with a selective COX-2 inhibitor during EtOH drinking prevented the changes in microglia, and attenuated the increase in cleaved caspase-3, and decreases in TH and DAT after Meth administration. Furthermore, motor dysfunction measured by a rotarod test was evident but only in rats that were exposed to both EtOH and Meth. The motor dysfunction was ameliorated by prior inhibition of COX-2 during EtOH drinking. The exaggerated neurochemical and behavioral deficits indicate that the comorbidity of EtOH and Meth induces a degeneration of the nigrostriatal pathway and support the role of inflammation produced by EtOH drinking that primes and mediates the neurotoxic consequences associated with the common co-morbidity of these drugs.

1. Introduction

Methamphetamine (Meth) users often display co-morbidities with other drugs such as alcohol. [Stinson et al. \(2005\)](#) revealed that upwards of 80% of amphetamine abusers have been diagnosed with an alcohol use disorder. Additionally, alcohol drinking typically precedes amphetamine use ([Leslie et al., 2017](#)) and increases the probability of Meth use by over 4-fold ([Bujarski et al., 2014](#)). It has been suggested that the two drugs in combination produce a greater euphoria, enhance performance and alleviate sleep disruptions, but can also lead to long-term behavioral and cognitive deficits ([Kirkpatrick et al., 2012](#); [Loxton and Canales, 2017](#)). Despite this high rate of co-abuse and negative behavioral consequences, few studies have identified the neurochemical effects of their combined exposure.

Inflammation is also a consequence of the combined exposure to alcohol and Meth. Rats allowed to freely drink ethanol (EtOH) exhibit increased serum lipopolysaccharide (LPS), a gut-derived endotoxin, that is released into circulation upon GI tissue insult to promote inflammation in the periphery and the brain ([Blaker and Yamamoto, 2018](#)). LPS signaling elicits the induction of pro-inflammatory mediators such as cyclooxygenase-2 (COX-2), a known contributor to

neuronal toxicity ([Crews et al., 2007](#)). Furthermore, LPS signaling induces changes in microglial morphology that are commonly associated with an inflammatory response ([Chen et al., 2012](#)). While alcohol can induce COX-2 expression in the brain ([Blaker and Yamamoto, 2018](#); [Knapp and Crews, 1999](#)), and COX-2 has been implicated in the neurotoxicity of Meth ([Thomas and Kuhn, 2005](#)), microglial activation has also been observed after either alcohol or Meth ([He and Crews, 2008](#); [Sekine et al., 2008](#); [Thomas et al., 2004](#)).

The neurotoxicity of Meth is characterized by decreases in dopamine and its transporter (DAT) ([Volkow et al., 2001](#); [Wagner et al., 1980](#)). This neurotoxicity is enhanced by prior voluntary EtOH drinking to produce a greater than 90% depletion of dopamine in the striatum and loss of DAT immunoreactivity compared to either drug alone ([Blaker and Yamamoto, 2018](#)). Moreover, non-selective inhibition of COX1/2 during EtOH drinking blocked the enhanced dopamine depletions and transporter immunoreactivity in the striatum observed 7 days after EtOH + Meth ([Blaker and Yamamoto, 2018](#)).

The synergistic relationship between EtOH and Meth on the loss of dopaminergic innervations of the striatum suggests damage to dopamine soma in the substantia nigra pars compacta (SNpc) and a neuropathology similar to Parkinson's disease. Neurodegeneration of the

* Corresponding author at: Department of Pharmacology & Toxicology, 635 Barnhill Drive, MS A418, Indianapolis, IN 46202, USA.

E-mail address: brkyama@iu.edu (B.K. Yamamoto).

¹ Equal contribution.

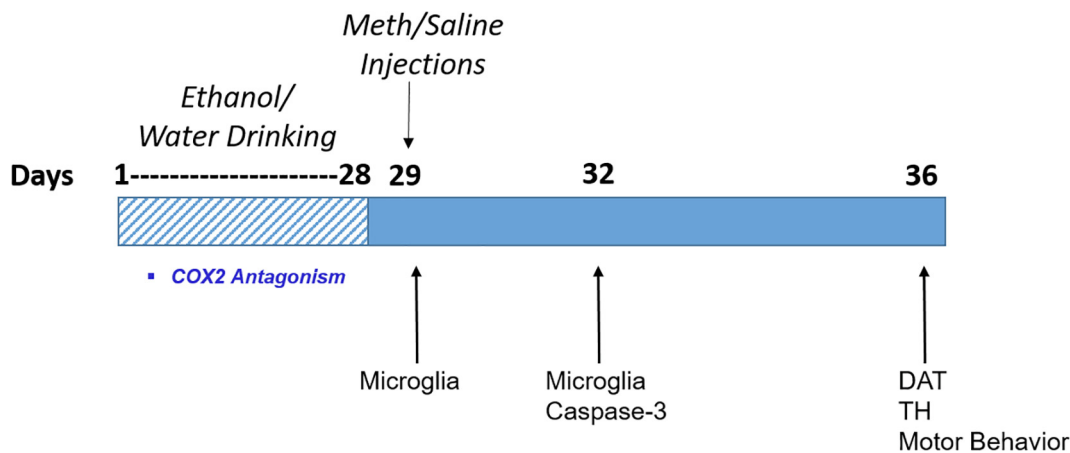


Fig. 1. A timeline describing the experimental paradigm and experimental measures.

nigrostriatal pathway can be mediated by apoptosis, one form of programmed cell death. Infusions of 6-OHDA into rats mimic this nigrostriatal degeneration and exhibits the pro-apoptotic markers cleaved caspase-3 and GSK-3 β prior to actual cell death (Hernandez-Baltazar et al., 2013). Additionally, the SNpc has the highest concentration of resident microglia in the brain (Lawson et al., 1990). Microglia make direct contact with dopaminergic cell bodies to promote microglial phagocytosis of neurons in the SNpc (Barcia et al., 2004; Barcia et al., 2012). Therefore, microglia are uniquely positioned to play a role in dopamine neuron degeneration but their response to the interactions between EtOH and Meth is unknown.

We examined the effects of voluntary EtOH drinking by rats prior to Meth administration on morphological changes in microglia that precedes a loss of a dopamine phenotype in the SNpc and the eventual appearance of motor deficits. Furthermore, we administered the COX-2 inhibitor nimesulide during EtOH drinking only, to identify a role for EtOH-induced inflammation in mediating the neurotoxic effects of the serial exposure to EtOH and Meth.

2. Materials and methods

2.1. Animals

Male Sprague Dawley rats (250–350 g, Envigo, Indianapolis, IN) were allowed to acclimate to the animal facility at Indiana University for approximately 7 days prior to experimentation. Rats had ad libitum access to food and water throughout all experiments. All experiments were carried out in accordance with the National Institutes of Health Guide for the Care and Use of Laboratory Animals as well as the Indiana University Institutional Animal Care and Use Committee.

2.2. Drug administration

Upon acclimation to the animal colony, rats were housed individually to measure EtOH consumption. Rats had intermittent access to 10% EtOH drinking for 28 days. In addition to a water bottle, an EtOH bottle was placed on each cage every other day for 24 h over a 28 day period as described in Li et al. (2011). When EtOH was not present, a second water bottle was placed on the cage to allow for a 2-bottle choice at all times. The positions of the bottles were switched daily to prevent side bias. Rats, EtOH bottles, and water bottles were weighed daily to measure the quantity of EtOH (g) consumed. EtOH intake was normalized to body weight (kg).

Rats were then exposed to a binge regimen of Meth (10 mg/kg, i.p.) injected once every 2 h for a total of 4 injections on the day after the last day of EtOH drinking. (+) Methamphetamine-hydrochloride (Sigma, St. Louis, MO, cat# M-8750) was dissolved in 0.9% saline. Saline (0.9%

NaCl, 1 mL/kg, i.p.) was used as a vehicle. This injection paradigm approximates the neurotoxicity (i.e., loss of DAT) observed in human Meth users (McCann et al., 1998; Volkow et al., 2001). The investigator-administered Meth paradigm permitted a clear interpretation of the pharmacological effects of Meth and controlled for a specific dose of Meth over a discrete period of time that is not easily feasible during the acquisition period and training needed in a Meth self-administration paradigm.

Body temperatures were monitored throughout the binge Meth exposure via subcutaneously implanted transponders (IPTT-300 transponder, BMDs). Temperature transponders were implanted on the last day of EtOH or water drinking. During the binge Meth or saline regimen, temperatures were measured remotely every 30 min. Use of these transponders circumvented the stress response that may arise from obtaining temperatures rectally.

To identify the effects of COX-2 inhibition during EtOH drinking, a subset of rats received nimesulide, a COX-2 selective inhibitor, throughout the 28 day EtOH drinking period. Nimesulide was obtained from Cayman Chemical (Ann Arbor, MI, cat#70640), dissolved in 0.9% saline, and administered at a dose of 7.5 mg/kg, i.p. twice daily on the days without EtOH access in order to block the EtOH-induced inflammation. This treatment dosage was based on the pharmacokinetic/pharmacodynamic properties of the drug (Ramesh et al., 2015; Taniguchi et al., 1997), specificity for COX-2 inhibition (Famaey, 1997) and was used in recent studies of the COX-2 mediated response to psychostimulants in rats (Anneken et al., 2013). Control injections were 0.9% saline (1 mg/mL) vehicle.

A timeline of the experimental paradigm and measurements is included in Fig. 1. Rats were allowed intermittent access to 10% EtOH for 28 days, during which a subset of rats were administered nimesulide (2.2). On the 29th day, rats underwent the binge Meth regimen and microglial morphology (2.3, 2.4) was assessed in the SNpc and striatum at 2 h after the last Meth injection. Three days after Meth administration, microglial morphology in the SNpc and striatum was assessed and cleaved caspase-3 (2.5) was measured in the SNpc. Seven days after Meth administration, striatal DAT immunoreactivity (2.6), TH-positive cell counts in the SNpc (2.5), and motor behavior (2.7) were assessed.

2.3. Immunohistochemistry

To identify the response of microglia to the serial exposure to EtOH and Meth, immunohistochemistry was used to visualize changes in microglial morphology at 2 h and 72 h after the last injection of Meth. Two or 72 h after the Meth binge and following blood collection from the heart, heparin (35 USP units) was injected into the left ventricle followed by the transcardial perfusion of 0.1 M phosphate-buffered saline (PBS) and then 4% paraformaldehyde (PFA). Brains were further

post-fixed in 4% PFA for 24 h, cryoprotected in glycerol solutions (24 h in 10% followed by 24 h in 20%), and flash frozen. Serial coronal sections (40 μm) were performed through the midbrain containing the SNpc (Bregma -4.8 through -6.04) or striatum (Bregma 1.6 through 0.2) from frozen brains using a cryostat (Cryostar NX7; Thermo Scientific, Waltham, MA). Three sections were collected per rat (one section was collected every 120 μm) for microglial staining. Sections were mounted onto gelatin-coated slides and probed for microglia using a polyclonal rabbit anti-ionized calcium-binding adaptor molecule – 1 antibody (Iba-1, 1:1000; Wako, Richmond, VA. cat #019-19741). Sections (40 μm) immediately adjacent to the section for microglial staining were stained for dopaminergic neurons of the SNpc with a rabbit monoclonal anti-tyrosine hydroxylase antibody (TH, 1:1000; Millipore Corp, MA. cat #AB152) to verify that all sections were in the same plane at the level of the SNpc. Staining was performed using immunohistochemical methods. Dry mounted sections were subjected to citrate buffer-mediated antigen retrieval (90 °C for 14 min), then washed with phosphate buffered saline (PBS; 3 \times 5 min). Endogenous peroxidases were inactivated by incubation with 1% H_2O_2 for 10 min. The sections were then washed with PBS (5 \times 5 min) and blocked for 2 h in normal goat serum (NGS; 3%) containing avidin blocking reagent (4 drops/mL block solution; Vector Laboratories, Burlingame, CA. cat #SP-2001) in PBS. This was followed by incubation overnight to 48 h at 4 °C in a solution containing the respective primary (1°) antibody and the biotin blocking reagent (4 drops/mL 1° antibody solution). Sections were then washed with PBS (5 \times 5 min), incubated for 1 h with biotinylated anti-rabbit antibody (1:1000; Vector Laboratories, Burlingame, CA. cat #BA-2000), washed with PBS (5 \times 5 min), and incubated for 2 h with Vectastain ABC Kit (Vector Laboratories, Burlingame, CA. cat #PK6100), according to the manufacturer's instructions. Staining was visualized using 3,3'-diaminobenzidine and urea-hydrogen peroxide tablets (Sigma-Aldrich, St. Louis, MO. cat #D4293). Sections were dehydrated using a graded series of ethanol, followed by incubation in xylenes to clarify the tissue, and then sealed under a cover slip using DPX mounting medium (Electron Microscopy Sciences, Hatfield, PA. cat #13510). Slides were analyzed by an experimenter blind to the treatment conditions.

2.4. Quantitation of Iba-1 immunoreactive cells in the SNpc using the Cell Profiler image analysis software

The Cell Profiler image analysis software was used to quantify the changes in the soma of populations of microglia. Images were captured using a Leica DM6 B light microscope (Leica Microsystems, Germany). Three images were analyzed per section. The particular region of interest that contains the SNpc with minimal overlap from the substantia nigra pars reticulata or other neighboring regions was first identified at 5 \times magnification, and marked with a square (0.33 mm \times 0.33 mm). The extended depth of field image was calculated and captured at 20 \times magnification. The Cell Profiler cell image analysis software (version 2.2.0, Broad Institute of Harvard and MIT, Cambridge, MA) was used to quantify both the number of Iba-1 immunoreactive cells and the two dimensional area of their identified cell bodies. Cell Profiler image analysis software permitted the quantification of cell soma size of a fairly large population of cells in a quick and efficient manner without the need for reconstruction of the cells (Carpenter et al., 2006). The pipeline used for these analyses was composed of the following modules: 1) RunImageJ to Auto-contrast and Sharpen images, 2) ImageMath to Invert (binarize) images and modify signal intensity, 3) Smooth (i.e., Smooth Keeping Edges) to enhance cell edges, 4) IdentifyPrimaryObjects to identify stained cells' soma, 5) MeasureNeurons to calculate the identified cells' soma sizes, 6) ExportToSpreadsheet to extract the data. Primary objects were identified by setting the diameter of objects > 20 and Threshold set at Global using the RidlerCalvard method with automatic smoothing. Intensity was used to distinguish clumped objects and threshold correction factor was established for each stained

cohort to account for batch-to-batch variability in staining. The same parameters were used for all rats within a given cohort. Identified cell counts and cell soma were compared across treatment conditions based on an area threshold of being greater than or equal to 75 μm^2 . The threshold chosen corresponds to measurements of microglial soma reported elsewhere (Kozłowski and Weimer, 2012; Torres-Platas et al., 2014).

2.5. Immunofluorescence

To determine the loss of TH positive cells at 3 and 7 days after the serial exposure to EtOH+Meth, immunofluorescence was used to quantify cell count in the SNpc. Three or seven days after the Meth binge, rats were anesthetized with ketamine (75 mg/kg) and xylazine (5 mg/kg) cocktail, i.p. Heparin (35 USP units) was injected into the left ventricle of the exposed heart and 0.1 M phosphate-buffered saline (PBS) followed by 4% paraformaldehyde (PFA) were transcardially perfused. Brains were cryoprotected in 10% glycerol at 4 °C overnight, 20% glycerol at 4 °C the following night, flash frozen, and sectioned at a thickness of 40 μm through the substantia nigra (Bregma -4.8 through -6.04) before mounting onto subbed slides to be stored at -20 °C.

The sections were washed 3 \times 10 min in 1X PBS and blocked for 1 h in 1X PBS containing 10% normal goat serum while gently shaking at room temperature. To visualize cleaved caspase-3 and dopamine cells, sections were incubated in primary antibodies for anti-cleaved caspase-3 (1:300, Cell Signaling cat#9664L) and anti-tyrosine hydroxylase (1:500, Millipore cat#MAB318). In a separate set of experiments to visualize dopamine and DAPI, sections were incubated in primary antibody for anti-tyrosine hydroxylase (1:1000, Millipore cat#AB152) alone overnight with shaking at 4 °C. The next day, all sections (both experiments) were washed 3 \times 10 min in 1X PBS and incubated in the appropriate secondary antibodies (1:3000, goat anti-rabbit IgG Alexa fluor 633, Thermo Fisher cat#A-21071 or goat anti-mouse IgG Alexa fluor 488, Life Technologies cat#A-11001) for 1 h while shaking at room temperature in the dark. The sections were exposed to another series of washes (3 \times 5 min each) in 1X PBS, and DAPI (4 $\mu\text{g}/\text{mL}$, Sigma-Aldrich cat #D9542) was included in the last 5 min wash for slides previously incubated in anti-tyrosine hydroxylase primary antibody alone. Slides were coverslipped with Fluoromount-G (Fisher Scientific cat #17984).

Leica DM6 B light microscope (Leica Microsystems, Germany) and ImageJ software were used to capture and visualize cell bodies within the SNpc. Conditions were blinded to the experimenter to prevent bias. Average counts of cleaved caspase-3 + TH or TH + DAPI co-labeled cells per rat was recorded from 3 to 4 slices. TH + DAPI co-labeled cells were also analyzed in the VTA (Bregma -4.80 to -6.04 ; data not shown). Every third 40 μm slice was evaluated.

2.6. Western blotting

To determine the loss of DA phenotype in the striatum, western blot techniques were used to quantify the loss of DAT in the striatum at 7 days after the serial exposure to EtOH+Meth. Seven days after the Meth binge, rats were euthanized for DAT quantification in crude synaptosomal fractions. Synaptosomes were prepared from striata dissected upon ice, as described in Blaker and Yamamoto (2018). Homogenized tissue was diluted in Novex 4X LDS sample buffer, and 30 μg protein was loaded per well after total protein quantification via Bradford assay. Bis-Tris gels (4–12%) were used for gel electrophoresis at 150 V for 90 min, followed by transfer onto PVDF membranes at 28 V for 120 min. Membranes were blocked for 1 h at room temperature while shaking in 5% milk, and incubated overnight in primary antibody for DAT (1:1000, anti-goat, Santa Cruz cat#SC1433) at 4 °C. The following day, membranes were washed 3 \times for 5 min each with TBS containing 0.5% Tween (TBS-T) and incubated with secondary antibody (HRP-conjugated goat anti-rabbit IgG, 1:3000, Santa Cruz

cat#SC2004) for 1hr at room temperature. Membranes were then incubated in HyGlo-enhanced chemiluminescence and imaged with a FujiFilm LAS-4000 camera. Multi-Gauge V3.1 software was used to quantify band density and density was normalized against β -actin (1:3000, Millipore cat#MAB1501).

2.7. Motor behavior

Performance on a rotarod test was used to determine motor dysfunction at 7 days after the serial exposure to EtOH + Meth. Three days after the Meth binge, rats began training on the rotarod (IITC Life Science Inc., Woodland Hills, CA, part #755). Rats were subjected to 3 training days on the rotarod as reported by Ferguson and Cada (2004). Each training day consisted of 3 5-minute trials. Day 1 was at a speed of 20 rpm, and days 2–3 were at 25 rpm. If rats fell off the rod within the 5-minute trial period, they were immediately placed back on the rod for the duration of the 5 min to facilitate the learning of the task. On the 4th and final test day, rats were placed on the rod at a speed of 30 rpm and remained atop the spinning rod. The latency to fall off the rod was recorded. Rats were not placed back on the rod after falling off on the final test day.

2.8. Statistics

EtOH intake was analyzed using a one-way repeated measures ANOVA over four time points. Results from Cell Profiler analysis were compared using two-way ANOVA with Tukey post-hoc analyses.

For the DAT immunoreactivity, DAPI, TH and cleaved caspase-3 immunofluorescence, and rotarod experiments, a 2-way ANOVA was used for treatment groups without nimesulide (Nim) (factors: Water/EtOH and Meth/Saline). Another 2-way ANOVA was used to analyze DAT within Meth groups, and a Tukey post-hoc was used to compare EtOH + Meth + Nim to EtOH + Meth + Saline. Student's *t*-test was used to analyze the effect of Nim within EtOH + Meth groups (i.e., cleaved caspase-3, DAT, and motor behavior). All statistical analyses were performed with SigmaPlot 13.0 software (Systat Software, SigmaPlot for Windows). All data are presented as mean \pm SEM.

3. Results

3.1. Rats increase EtOH intake over 28 days

Grams of EtOH (or water control) consumed were normalized to body weight (kg). A repeated measures ANOVA showed that there was a significant increase in EtOH intake over the 28 days ($n = 97$; $p < 0.001$; Fig. 2). Rats drank 2.65 ± 0.16 g/kg/24 h on Day 1, 3.36 ± 0.20 g/kg/24 h on Day 14, 4.05 ± 0.21 g/kg/24 h on Day 21, and 4.45 ± 0.25 g/kg/24 h on the last day of access. EtOH drinking did not affect body weight compared to water drinking controls (Water: 323 ± 6.07 g vs. EtOH: 321 ± 8.03 g on Day 28). Additionally, nimesulide did not affect EtOH intake compared to vehicle-treated controls (data not shown).

3.2. Effects of EtOH drinking on Meth-induced hyperthermia

Body temperatures were monitored closely throughout the binge Meth regimen. A two-way repeated measures ANOVA with Tukey post hoc analyses showed no difference in hyperthermia between Water + Meth and EtOH + Meth groups (Fig. 3).

3.3. Iba-1 immunoreactive cells in the SNpc exhibit increases in number and soma size after EtOH + Meth that are attenuated by nimesulide intervention

The micrograph of TH-stained dopaminergic neurons in the SNpc shown in Fig. 4A illustrates the region of interest from where images of Iba-1 immunoreactive cells were taken. Fig. 4B includes a

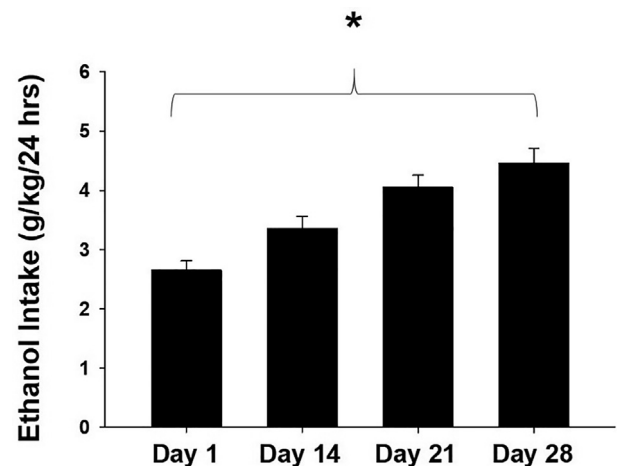


Fig. 2. Drinking behavior in Sprague Dawley rats over 28 days. Rats increased EtOH intake (g/kg/24 h) over time ($*p < 0.001$; $n = 97$). Data are presented as mean \pm SEM.

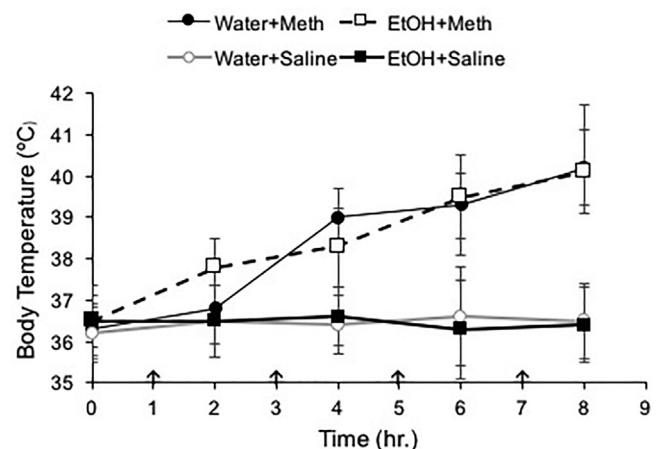


Fig. 3. Body temperatures during Meth administration. All rats treated with Meth displayed increases in body temperature over time, but previous EtOH drinking did not affect hyperthermia during Meth. Arrows denote injection times. Data are presented as mean \pm SEM.

representative image from Iba-1 immunoreactive cells within the SNpc for each treatment condition. Binary images at $20\times$ and individual cells at higher magnification ($40\times$) are included alongside color images to highlight the differences in morphology when comparing microglia from different treatment groups. Stained cells in the Water + Saline control and EtOH + Saline groups exhibit similar profiles in that their cell soma are mostly small, round, with projections that are thin and long, extending from the cell body without contact or overlap with neighboring cells. In contrast, microglia in the images from Water + Meth and EtOH + Meth groups exhibit larger and highly convoluted cell soma with increased branching complexity emerging from the soma (e.g., thicker processes with increased branch points), with EtOH + Meth group exhibiting the greatest changes. There is also a greater number of cells present in each of the images when compared to either Water + Saline or EtOH + Saline groups and seemingly greater overlap in the space occupied by their processes.

The effects of nimesulide treatment on these cells are evident in the representative images shown in Fig. 4C. There were no differences in degrees of staining between the nimesulide experiments and the non-nimesulide experiments with regard to the control groups. Nevertheless, all groups treated with nimesulide appear similar morphologically regardless of Meth and/or EtOH treatment.

Results from the analysis of the population of cells identified in each

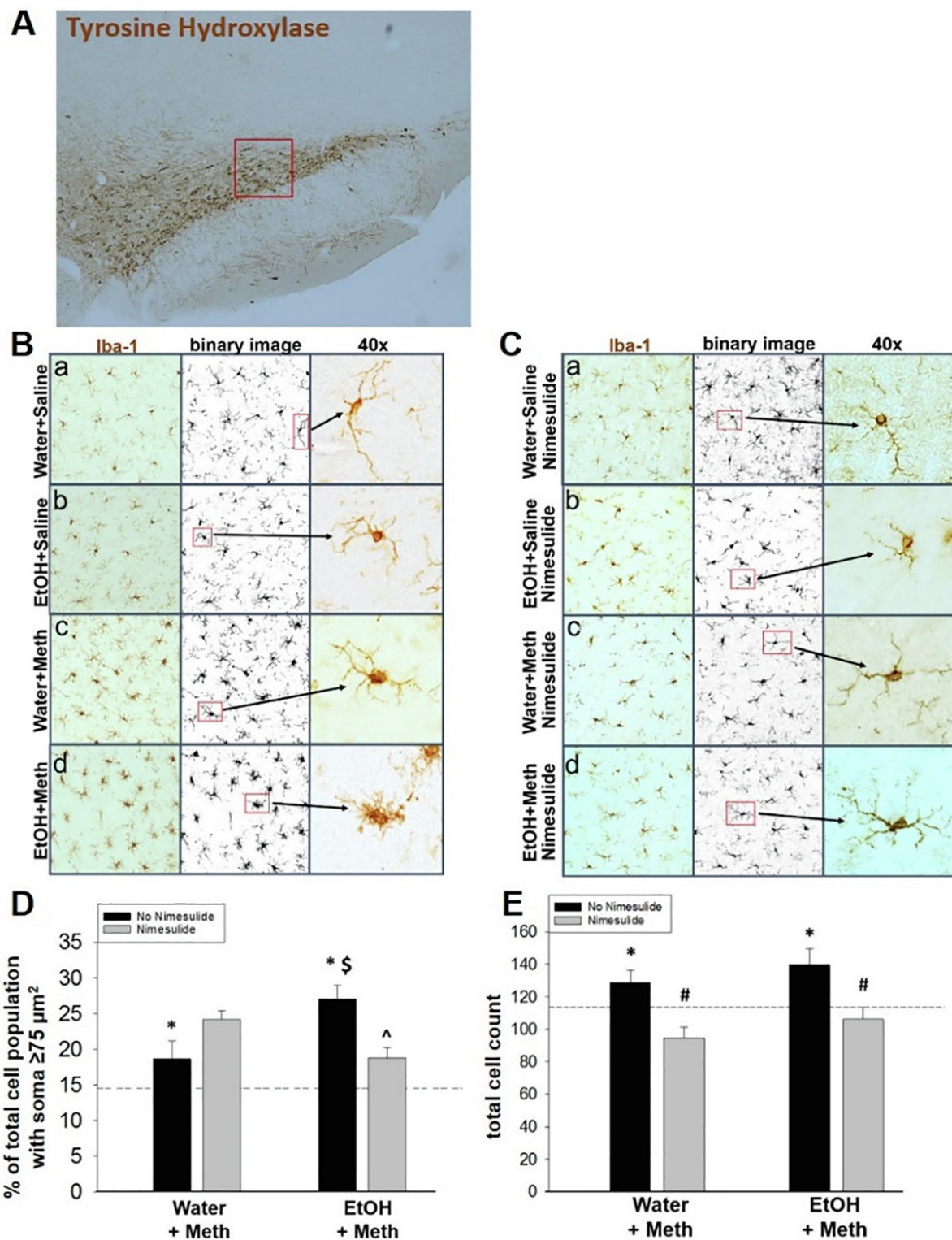


Fig. 4. EtOH + Meth changes morphology and number of Iba-1 immunoreactive cells 2hr after Meth and this is mediated by COX-2. A) The region of interest within the SNpc is outlined in red (5×). Representative images of Iba-1 immunoreactivity in rats with B) no nimesulide and C) nimesulide intervention during EtOH drinking. Images are at 20× and 40×. D) Meth-treated rats displayed significantly larger % of total cells with large cell bodies compared to saline-treated rats (n = 6–12/group, **p* < 0.05). This was further enhanced by EtOH (n = 3–12/group, [§]*p* < 0.05) and was blocked by nimesulide ([^]*p* < 0.05). E) Meth treatment significantly increased total number of microglia (n = 6–12/group, **p* < 0.05) and this was also blocked by nimesulide (n = 3–12/group, [#]*p* < 0.05). Results are presented as mean ± SEM. The dotted line represents the mean of the Water + No Nimesulide + Saline (D-E). (For interpretation of the references to color in this figure legend, the reader is referred to the web version of this article.)

treatment group are shown in Fig. 4D-E. The data presented in Fig. 4D are the mean percent of all cells identified (per rat) whose two-dimensional cell soma surface area was equal to or greater than $75 \mu\text{m}^2$. This threshold was chosen for comparison to correspond with measurements of microglial soma reported elsewhere (Kozłowski and Weimer, 2012; Torres-Platas et al., 2014). A 2-way ANOVA of cell soma size amongst animals that did not receive nimesulide revealed a significant overall Meth effect ($n = 6\text{--}12/\text{group}$; $*p < 0.05$) illustrating that Meth increased the percent of cells with soma $\geq 75 \mu\text{m}^2$. An analysis of Meth-treated rats identified a significant interaction (2-way ANOVA, Water/EtOH \times no nimesulide/nimesulide, $n = 3\text{--}12/\text{group}$, $p < 0.05$) that was due to the difference between Water+Meth and EtOH+Meth (Tukey post-hoc, $n = 3\text{--}12/\text{group}$, $^{\text{S}}p < 0.05$). A 2-way ANOVA analysis of the Meth treated groups with and without nimesulide revealed a significant interaction effect ($p < 0.01$) that was due to a 30% attenuation of increases in cell size in the EtOH+Meth group (Tukey post-hoc test, $n = 3\text{--}12/\text{group}$, $\hat{p} < 0.05$).

An analysis of the total cell counts in each treatment group, with and without nimesulide, are shown in Fig. 4E. The groups that did not receive nimesulide showed a significant effect of Meth (2-way ANOVA, Water/EtOH vs. Sal/Meth, $n = 6\text{--}12/\text{group}$; $*p < 0.01$) on increasing total cell counts. A comparison within Meth treated groups revealed a significant nimesulide effect (Water/EtOH \times no nimesulide/nimesulide, $n = 3\text{--}12/\text{group}$, $p < 0.01$) that was due to a decrease in total cell number in the Water+Meth and EtOH+Meth groups (i.e., 25% and 24%, respectively) by nimesulide intervention (Tukey post-hoc,

$n = 3\text{--}12/\text{group}$, $\#p < 0.05$).

The representative micrographs in Fig. 5A indicate that changes in microglial morphology observed at 2 h in the SNpc are no longer evident at 72 h after the Meth binge. The cells identified in these treatment groups are similar to each other (e.g., small rounded cell bodies with thin and long processes), and resemble those of the control cells (i.e., Water+Saline) identified at 2 h after the Meth binge (Fig. 4B). In agreement with this observation, quantitative analysis of the identified cells (Fig. 5B-C) shows similar results in the measurements of soma size and number of all cells identified. Statistical analysis of these results indicated no significant difference between groups for either measure of soma size or number of cells. Nimesulide during EtOH drinking had no effect on body temperature in EtOH+Meth rats during Meth (average over time for EtOH+Meth+Saline: $38.14 \pm 1.92^\circ\text{C}$ vs. EtOH+Meth+Nimesulide: $38.36 \pm 3.33^\circ\text{C}$).

3.4. Iba-1 immunoreactive cells in the striatum exhibit no changes in number and soma size at 2 h or 72 h

Representative micrographs of microglia from the striatum are shown in Fig. 6. Although cells in this region are generally larger than those observed in the SNpc, an analysis of microglia in the striatum at 2 h and 72 h after the last Meth injection shows no observable (Fig. 6A-B) or quantifiable (Fig. 6C-D) changes in microglia size due to EtOH, Meth, or the combination.

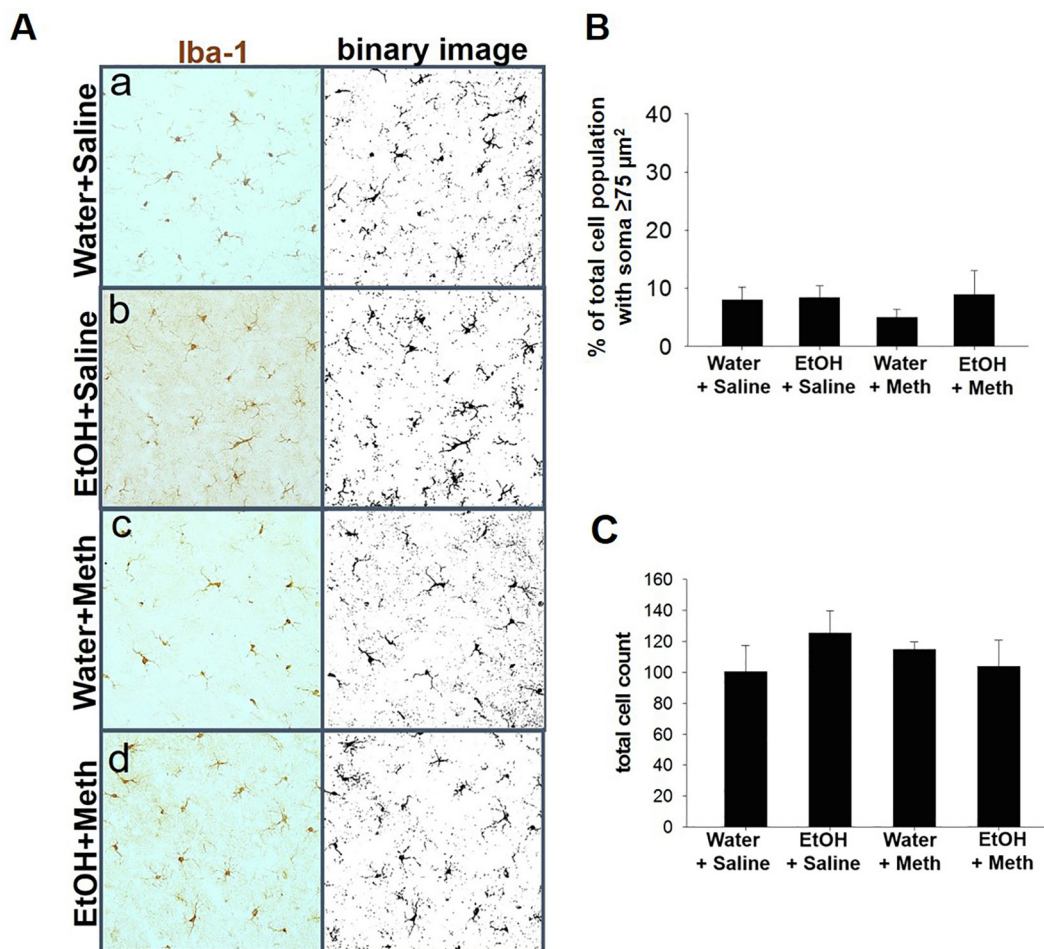


Fig. 5. Iba-1 immunoreactive cells of the SNpc lose morphological complexity 72 h post Meth binge. A) Representative images of Iba-1 stained sections from animals at 72 h post Meth binge from a) Water+Saline, b) EtOH+Saline, c) Water+Meth, and d) EtOH+Meth treatment groups. Images are at 20x. B-C) Analysis of Iba-1 stained cells within the SNpc at 72 h post Meth binge indicates that changes in B) cell soma size measurements, and C) the total number of cells identified at 2 h, are no longer present. $n = 3\text{--}6/\text{group}$.

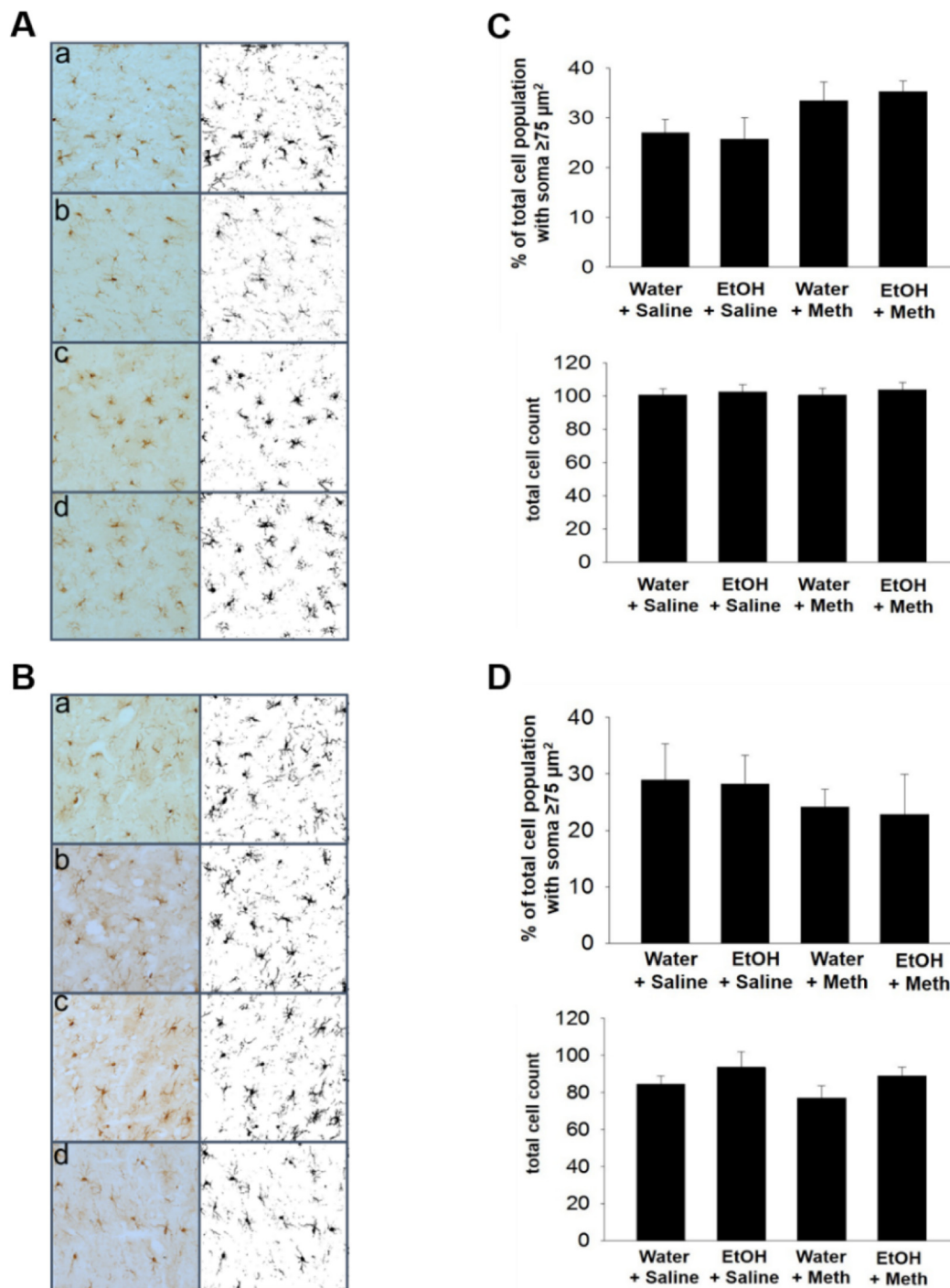


Fig. 6. Iba-1 immunoreactive cells of the striatum show no changes in morphology after treatment. Representative images of Iba-1 stained striatal sections from animals at A) 2 h and B) 72 h post Meth binge from a) Water + Saline, b) EtOH + Saline, c) Water + Meth, and d) EtOH + Meth treatment groups are shown. Analysis of Iba-1 stained cells in the striatum at C) 2 h and D) 72 h post Meth binge indicates no effect of EtOH, Meth, or the combination, at these time points. Results are presented as mean \pm SEM. $n = 3\text{--}12/\text{group}$.

3.5. Nimesulide during EtOH blocks EtOH + Meth-induced decreases in DAT immunoreactivity in the striatum

Seven days after Meth, a 2-way ANOVA showed a significant decrease in DAT in Meth-treated vs. saline-treated rats ($n = 6\text{--}8/\text{group}$; $p < 0.05$; Fig. 7A) with a synergistic decrease in rats previously exposed to EtOH (Tukey post hoc; EtOH + Meth vs. Water + Meth; $p < 0.05$). A subset of rats was treated with nimesulide or saline vehicle during EtOH drinking, and a 2-way ANOVA within Meth-treated

groups revealed a significant interaction between EtOH and nimesulide ($p < 0.05$; Fig. 7B). Nimesulide treatment blocked the enhanced decreases in DAT immunoreactivity in EtOH + Meth rats ($n = 5\text{--}7/\text{group}$; Tukey post hoc; EtOH + Saline + Meth vs. EtOH + Nim + Meth; $p < 0.05$). A representative Western blot is shown in Fig. 7C. Nimesulide alone did not affect DAT in the striatum (data not shown).

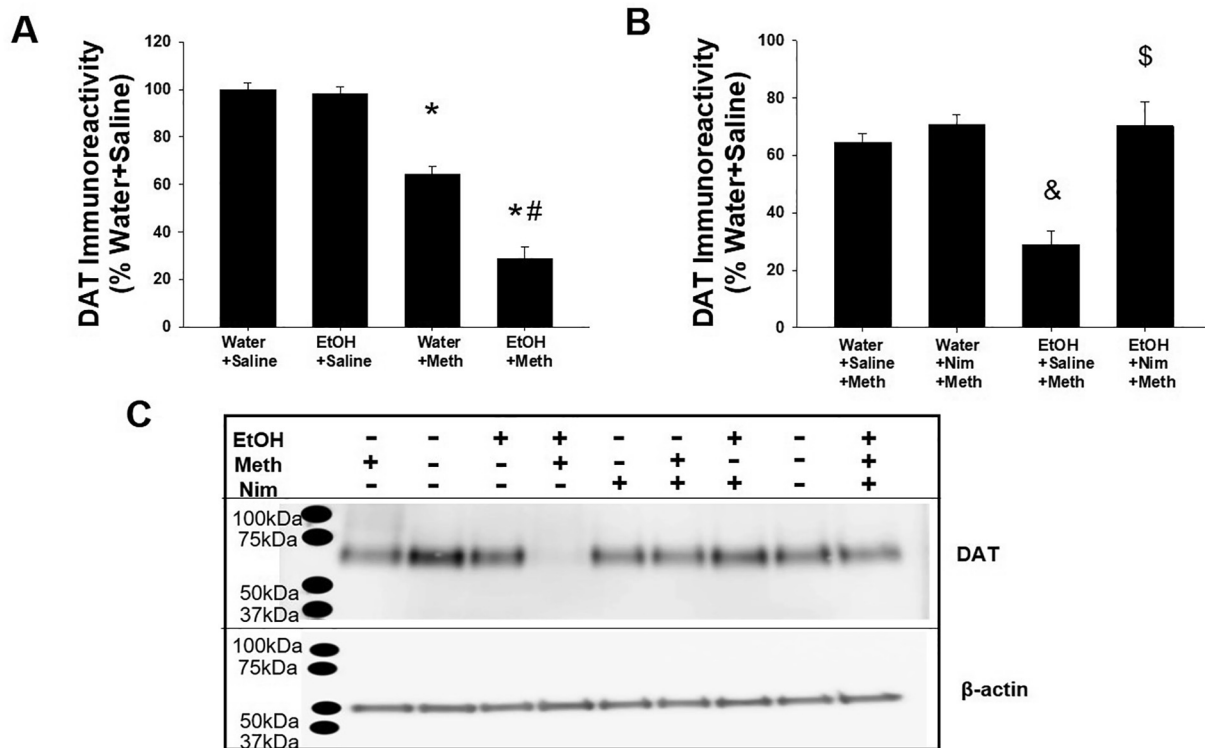


Fig. 7. COX-2 inhibition during EtOH drinking prevents enhanced Meth-induced DAT depletions. A) DAT was significantly decreased in Meth-treated vs. saline-treated rats ($n = 6-8/\text{group}$; $*p < 0.05$) and further decreased in rats previously exposed to EtOH ($^{\#}p < 0.05$ vs. Water + Meth). B) Nimesulide treatment during EtOH drinking blocked the synergistic decreases in DAT after EtOH + Meth ($n = 6-8/\text{group}$; $^{\&}p < 0.05$ vs. Water + Saline + Meth; $^{\$}p < 0.05$ vs. EtOH + Saline + Meth). C) Representative image of Western blot for DAT with β -actin as the loading control.

3.6. EtOH + Meth does not affect TH immunoreactivity at 3 days, but decreases TH immunoreactivity in the SNpc 7 days after Meth

Three days after Meth, there were no differences between groups in the number of TH-positive cells in the SNpc (data not shown). However, 7 days after Meth, a 2-way ANOVA showed a significant interaction between EtOH and Meth ($p < 0.001$). The EtOH + Meth rats showed a significant decrease in TH-positive cells compared to Water + Meth (Tukey post-hoc analyses, $n = 6-8/\text{group}$; $p < 0.01$, Fig. 8F). A subset of rats included those treated with nimesulide during EtOH drinking. There was a significant difference in TH-positive cells 7 days after Meth from those treated and not treated with nimesulide (EtOH + Meth + Nimesulide vs. EtOH + Meth, $n = 6-8/\text{group}$, $p < 0.05$). Additionally, nimesulide alone did not affect Meth-induced hyperthermia compared to vehicle-treated controls ($39.68 \pm 0.93^\circ\text{C}$ and $39.26 \pm 0.85^\circ\text{C}$, respectively). Representative images are shown for each treatment group at 5X magnification. The 20X inset points to TH-positive cells with DAPI fluorescence (Fig. 8A-E). TH + DAPI co-labeled cells were also quantified in the VTA, but no differences were observed between groups (data not shown).

3.7. Loss of TH immunoreactivity in the SNpc of EtOH + Meth is preceded by cleaved caspase-3

Three days after Meth, a two-way ANOVA with Tukey post hoc analyses showed a significant increase in the pro-apoptotic marker cleaved caspase-3 in TH-positive cells within the SNpc after EtOH + Meth (vs. all groups, $p < 0.05$, $n = 5-8/\text{group}$, Fig. 9A). The number of cleaved caspase-3 + TH co-labeled cells in EtOH + Saline and Water + Meth groups did not differ from the Water + Saline group. A subset of rats was treated with nimesulide during EtOH drinking and a t -test revealed that nimesulide attenuated the activation of cleaved caspase-3 in EtOH + Meth rats ($p < 0.05$, $n = 5-7/\text{group}$, Fig. 9B).

3.8. EtOH + Meth leads to motor deficits, which are attenuated by nimesulide treatment

Three days after Meth, rats began training for a rotarod test. On the final test day (7 days after Meth), a 2-way ANOVA showed a significant interaction between EtOH and Meth ($n = 8-14/\text{group}$; $p < 0.001$; Fig. 10A). Rats exposed to EtOH + Meth displayed a shorter latency to fall compared to all other groups (Tukey post-hoc test, $p < 0.001$ vs. Water + Meth). Nimesulide treatment during EtOH drinking attenuated the decreased latency to fall in EtOH + Meth rats (Student's t -test, EtOH + Meth + Saline vs. EtOH + Meth + Nimesulide, $p < 0.05$; $n = 8-9/\text{group}$; Fig. 10B). Nimesulide alone did not affect motor function (data not shown).

4. Discussion

EtOH drinking intermittently over 28 days followed by a binge Meth exposure produced synergistic changes in microglial morphology. These changes preceded long-term decreases in TH immunoreactivity in the SNpc and DAT in the striatum, both of which were paralleled by motor deficits. Co-administration of the COX-2 inhibitor, nimesulide, during EtOH drinking only, attenuated the loss of dopamine phenotype and motor dysfunction after EtOH and Meth exposure. These findings provide evidence for a novel, synergistic neurotoxicity in a brain region not typically damaged by either drug alone that is mitigated by COX-2 antagonism.

The finding that rats voluntarily increased their drinking of 10% EtOH over 28 days is consistent with published literature (Li et al., 2011; Simms et al., 2008). Although no changes were seen in microglial morphology in the striatum or the SNpc after EtOH drinking, increases in COX-2 expression in the striatum after EtOH drinking have been reported (Blaker and Yamamoto, 2018). Previous reports of increases in LPS in serum and brain are indicative of a gut-brain interaction (Blaker

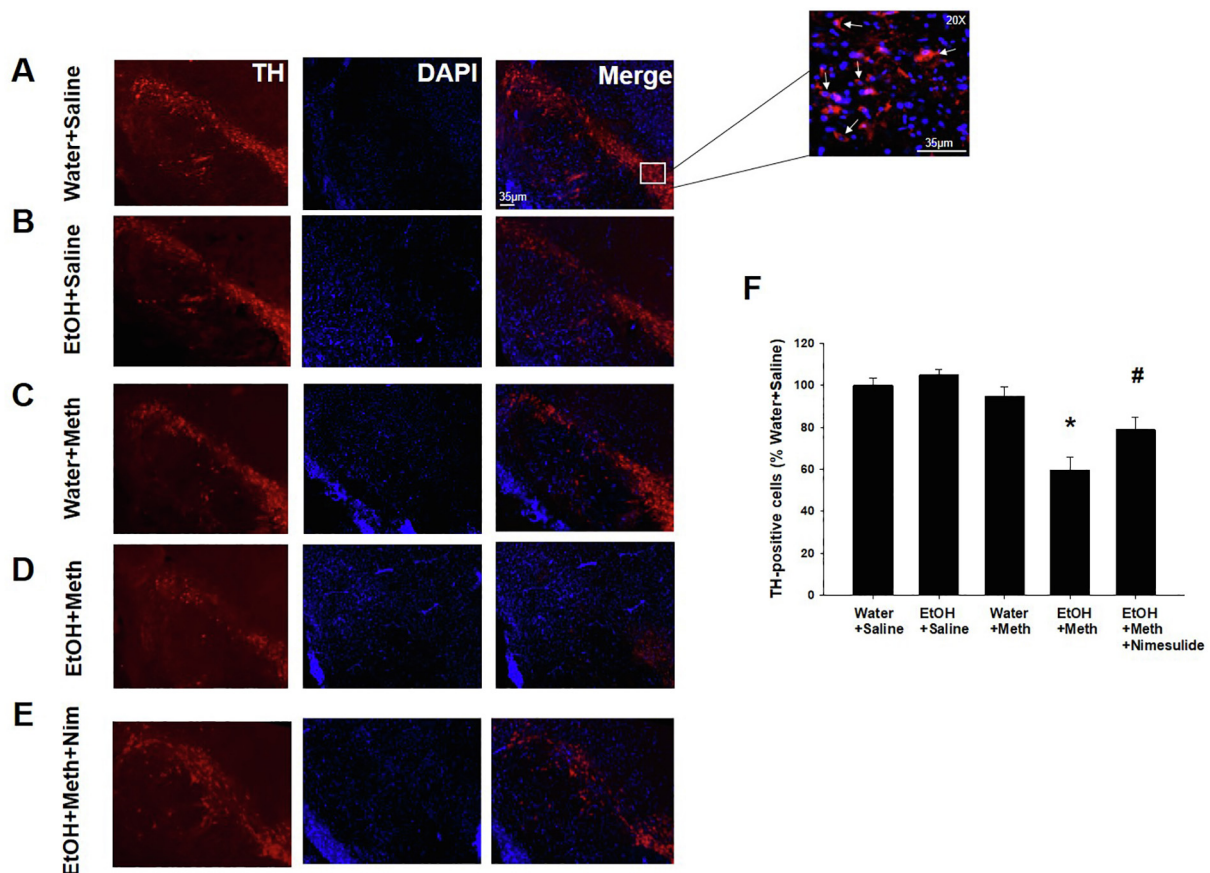


Fig. 8. TH+immunoreactivity is decreased in the SNpc 7 days after EtOH+Meth. TH+immunoreactivity in the SNpc is shown in A) Water+Saline, B) EtOH+Saline, C) Water+Meth, D) EtOH+Meth, and E) EtOH+Meth+Nim treatment groups. F) EtOH+Meth rats displayed significantly less TH+cells than all other groups ($n = 6-8/\text{group}$; $*p < 0.05$). Meth rats treated with nimesulide during EtOH drinking did not show the same extent of decreased TH-positive cells in the SNpc compared to EtOH+Meth ($^{\#}p < 0.05$). Data are expressed as mean \pm SEM.

and Yamamoto, 2018). LPS has been shown to induce an upregulation of COX-2, increase cytokines such as IL-1 β that activate macrophages, including microglia (Kaushik et al., 2013), and contribute to chronic neurodegeneration similar to that observed in Parkinson's disease (Koprach et al., 2008; Levi et al., 1998; Vijitruth et al., 2006). Furthermore, EtOH has been shown to induce COX-2 in the rat brain, but the cellular location is unknown (Knapp and Crews, 1999). In addition, the induction of COX-2 in TH-positive cells in the SNpc has been reported in a mouse model of PD in response to MPTP, and was shown to contribute to the loss of DA phenotype in the SNpc (Teismann et al., 2003)

Cyclooxygenases are necessary for the synthesis of prostaglandins that can effect microglial responses, including phagocytosis (Johansson et al., 2015) and the production of cytokines and reactive oxygen species (Quan et al., 2013). Additionally, COX-2 catalyzes the formation of dopamine quinones capable of activating microglia (Hastings, 1995; Kuhn et al., 2006) and has been implicated in the damage to dopaminergic terminals in the striatum produced by Meth (Thomas and Kuhn, 2005). Likewise, COX-2 has been implicated in the pathogenesis of Parkinson's disease such that cyclooxygenase inhibitors have a protective effect against the onset of idiopathic Parkinson's disease (Rees et al., 2011; Teismann, 2012). Similarly, the non-selective COX inhibitor, ketoprofen, attenuated decreases in dopamine phenotype in the rat striatum after serial exposure to EtOH and Meth (Blaker and Yamamoto, 2018). The current work illustrates that the protective effect of ketoprofen was likely due to the inhibition of COX-2 during EtOH drinking, as the selective COX-2 inhibitor, nimesulide, protected against the loss of dopaminergic cells in the SNpc and resultant motor dysfunction, while also reducing the microglial response in the SNpc (Fig. 8F, 10B and 4, respectively). While the protective effect of

nimesulide is presumed to occur via inhibition of prostaglandin signaling, COX-2 inhibitors have also been shown to inhibit the production of ROS which may contribute to neuronal toxicity (Teismann et al., 2003).

The increase in microglial soma size produced by Meth was enhanced by prior exposure to EtOH (Fig. 4D) and indicates activation of microglia as increases in cell size are positively correlated with increased activation (Marinova-Mutafchieva et al., 2009). However, it is important to note that changes in microglia do not indicate a distinct mechanistic or inflammatory consequence (i.e. phagocytic, pro- or anti-inflammatory). As changes in morphology are only an indicator of activation, other measurements are needed to determine a more defined role for microglia (e.g., upregulation of cytokines, oxidases, reactive oxygen species, etc.). Although EtOH drinking alone did not elicit measurable changes in soma size or number, it is associated with increases in serum LPS (Blaker and Yamamoto, 2018), which can activate microglia (Hoogland et al., 2015). The changes in microglial morphology exhibited by exposure to Meth were mirrored by increases in microglia number, which unlike cell size, was not further increased statistically by prior exposure to EtOH. This finding suggests that microglial activation (i.e. cell size), rather than proliferation (i.e. cell number), produced by Meth is more sensitive to priming by EtOH drinking. The lack of microglial response in the striatum at either time point (i.e., 2 h and 72 h) was surprising considering previous studies that reported changes in microglial morphology in the striatum at 48 h after Meth administration (LaVoie et al., 2004). This observation, and the lack of response in the SNpc at 72 h, illustrates the highly transient nature of the microglial response.

To examine the role of EtOH in the priming of a pro-inflammatory

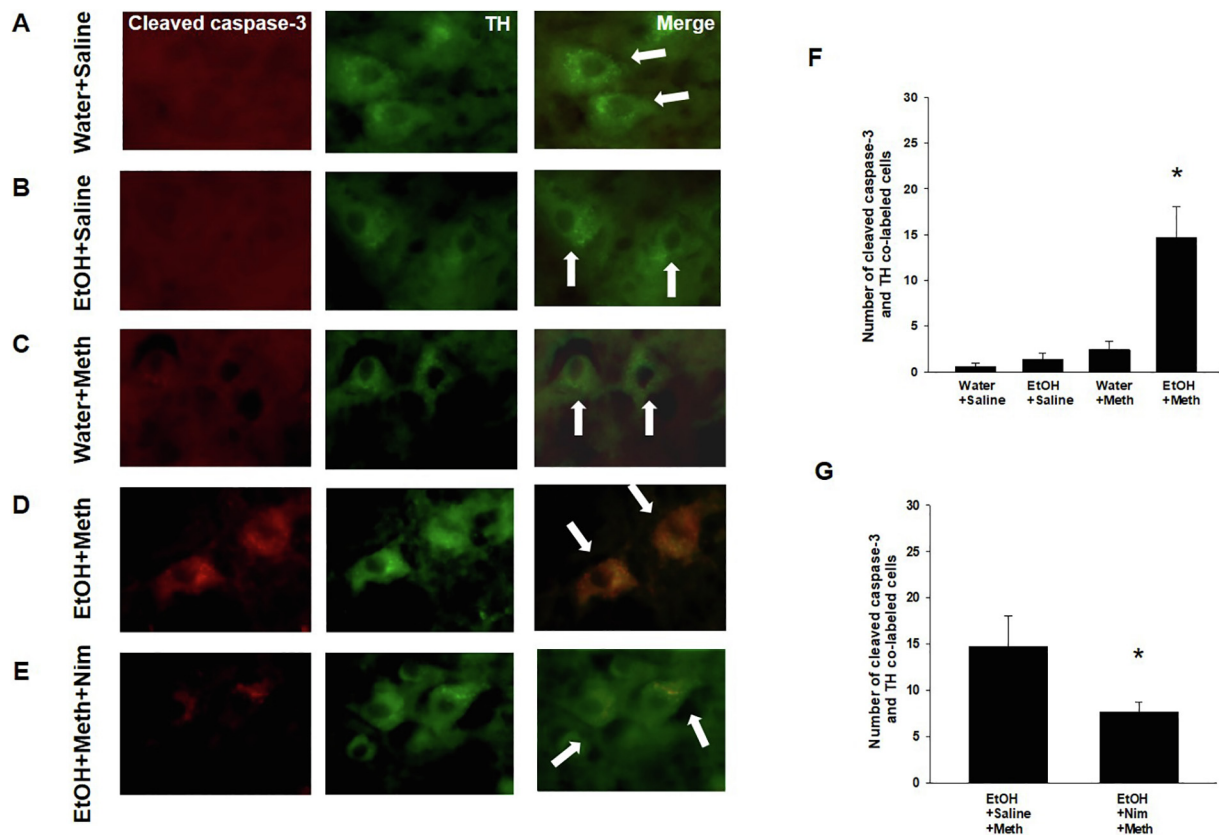


Fig. 9. EtOH + Meth induces apoptosis in dopaminergic neurons in the SNpc. Representative images for cleaved caspase-3 and TH immunofluorescence are provided for A) Water + Saline, B) EtOH + Saline, C) Water + Meth, and D) EtOH + Meth. F) EtOH + Meth significantly increased the number of cleaved caspase-3 and TH co-labeled cells in the SNpc (**p* < 0.05 vs. all groups). E) A subset of rats was treated with nimesulide during EtOH drinking and this attenuated the number of apoptotic cells in the SNpc (G). **p* < 0.05. *n* = 5–8/group. Data are represented as mean ± SEM.

state via upregulation of COX-2 in the brain prior to Meth exposure, nimesulide was administered to rats on the days without EtOH access throughout the 28 days of drinking. This anti-inflammatory regimen during these discrete time points permitted the targeting of EtOH-induced COX-2 activation independent of Meth-induced inflammation. The finding that nimesulide blocked the EtOH + Meth-induced increases in microglia number and cell size suggests an integral role for COX-2 in the microglia responses within the SNpc. The increase in cell size produced by Meth occurred only after prior exposure to EtOH and was

blocked by nimesulide whereas the increase in cell number produced by Meth alone was blocked by nimesulide regardless of prior exposure to EtOH. These results are consistent with the findings that prostaglandin signaling is known to mediate microglial activity (Johansson et al., 2015). Microglia at rest, play a largely homeostatic role in the CNS that includes surveillance of the brain parenchyma including phagocytosis and removal of damaged tissue and toxic molecules (Yin et al., 2017). Although microglial morphology can change after an inflammatory stimulus (e.g., by LPS) in the absence of neurodegeneration (Chen et al.,

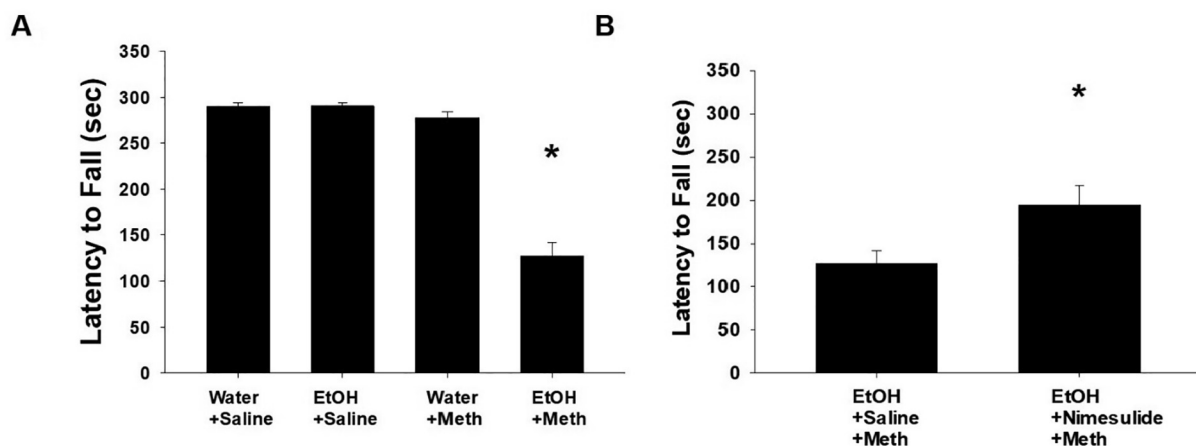


Fig. 10. EtOH + Meth decrease motor function at 7 days after Meth. A) 2-way ANOVA showed a significant interaction between EtOH and Meth (*n* = 8–14/group; *p* < 0.001). Tukey post-hoc analyses showed that EtOH + Meth rats fell off the rotarod sooner than their EtOH-alone or Meth-alone counterparts (**p* < 0.001). B) Rats treated with nimesulide in addition to EtOH + Meth did not exhibit motor deficits compared to the EtOH + Meth with saline vehicle (Student’s *t*-test; *n* = 8–9/group; **p* < 0.05).

2012), changes in morphology are commonly used as markers of an inflammatory response. Furthermore, the differential effects of nimesulide, and presumably prostaglandin signaling, on cell number vs. cell size in the absence of EtOH also suggest different mechanisms regulating changes in cell size and number produced by Meth alone. Regardless, the current study indicates that distinct mechanisms underlie microglial activation and proliferation produced by Meth alone and in combination with prior exposure to EtOH.

The morphological changes in microglia observed in the SNpc at 2 h after the Meth binge is no longer present at 72 h (Fig. 5). These early but transient changes precede the increases in apoptotic markers at 3 days and the eventual loss of TH immunoreactivity in the SNpc measured 7 days. The results are consistent with previous findings that Meth can damage dopamine soma in the SNpc of mice (Rumpf et al., 2017) and that microglial activation precedes terminal damage in the striatum (LaVoie et al., 2004). While further studies are required to identify a causal relationship between microglial activation and loss of dopamine integrity in the SNpc, it is important to note that the robust changes in microglial morphology are present only with serial drug exposure and mirror the dopamine cell loss in this region.

The finding that nimesulide blocked increases in microglia cell number and soma size in the EtOH + Meth groups provides evidence of COX-2-mediated damage to dopamine neurons and is consistent with the findings that COX-2 mediates Meth-induced striatal dopamine terminal degeneration (Thomas and Kuhn, 2005; Blaker and Yamamoto, 2018). The attenuation of increases in microglia cell number in Water + Meth groups indicates a contribution of basal prostaglandin signaling in Meth-induced changes to microglia in the SNpc. This does not preclude other mechanisms underlying microglia activation that could damage nigrostriatal dopamine neurons.

DAT immunoreactivity was decreased by 35% after Meth and was further decreased to 70% in rats that previously drank EtOH (Fig. 7A). This indicates a synergy between EtOH and Meth since EtOH alone did not decrease DAT. The changes in DAT are not due to hyperthermic or metabolic changes in rats exposed to EtOH + Meth such that EtOH drinking did not increase Meth-induced hyperthermia or change Meth concentration in the brain after previous exposure to EtOH (Fig. 3). Additionally, the synergistic nature of EtOH and Meth has been highlighted by studies showing a dose-dependent effect of EtOH consumption on subsequent Meth-induced monoamine depletions in the brain. The enhanced effect of EtOH on Meth-induced decreases in DAT were paralleled by decreases in TH immunoreactivity in the SNpc. The synergistic interaction between EtOH and Meth was more pronounced as neither EtOH drinking nor Meth decreased TH immunoreactivity compared to the 40% decrease produced by their serial exposure (Fig. 8F). DAT depletions in the striatum appear larger in magnitude compared to the loss of TH in the SNpc after EtOH + Meth. This can be explained by the fact that dopamine cell bodies in the SNpc give rise to multiple terminals in the striatum. Therefore, multiple terminals are lost with each cell body as revealed by a greater loss of DAT in striatum compared to TH-positive cell bodies in the SNpc (Figs. 7 and 8). In contrast to the lack of effect of Meth alone on SNpc TH in the current study, it has been reported that mice show a decrease in TH and cell damage in the SNpc after Meth (Ares-Santos et al., 2014). This difference is likely related to species differences between mice and rats in response to Meth. Nevertheless, the decrease in TH and DAT produced by EtOH + Meth was attenuated by nimesulide administration during EtOH drinking and indicates that COX-2 activation produced by EtOH can produce a sensitization or priming of the neurotoxic effects of Meth on TH and DAT. It remains to be determined if the decrease in DAT within the striatum precedes or is a consequence of the decreases in TH observed at 7 days after Meth. Regardless, no changes in TH were observed at 3 days after a Meth binge even though changes in microglia size and number occurred earlier (2 h).

Before the loss of TH + cells was observed in the SNpc, cleaved caspase-3 immunoreactivity was detected after EtOH + Meth (Fig. 9),

implicating a role for apoptosis in dopaminergic neuron death. This is consistent with previous studies suggesting apoptosis mediates nigral cell death in Parkinsonian rodent models as well as other models of dopaminergic neurodegeneration (Macaya et al., 1994; Naoi and Maruyama, 1999; Tatton and Kish, 1997). It is important to note that cleaved caspase-3 was not observed in *all* TH-positive neurons but was specific to dopamine cell bodies in the SNpc, as opposed to the VTA or SN pars reticulata (data not shown). Though negligible, we also observed faint cleaved caspase-3 immunoreactivity in the Water + Meth group when compared to EtOH alone or Water + Saline (Fig. 9C). This could be due to cellular injury from Meth, which may slightly activate cleaved caspase-3, but not lead to apoptosis (Cheng and Zochodne, 2003). However, based on the extent of dopamine neurons positive for cleaved caspase-3 staining at 3d after Meth in only the EtOH + Meth group (Fig. 9D) and the subsequent loss of TH + cells at a later time point (Fig. 8), the loss of TH immunoreactivity after EtOH + Meth is likely due to apoptosis.

Finally, the COX-2 inhibitor nimesulide during EtOH drinking only attenuated the number of apoptotic neurons as evidenced by cleaved caspase-3 and less dense staining of cleaved caspase-3 in TH-positive neurons of the SNpc after Meth exposure. These results are consistent with evidence for a role of COX-2 in the apoptosis of dopamine neurons (Sánchez-Pernaute et al., 2004; Vijitruth et al., 2006).

The neurochemical effects that we observed in the SNpc and striatum were paralleled by motor impairments (Fig. 10). Similar to the prevention of loss of TH in the SNpc (Fig. 8F), DAT in the striatum (Fig. 7A), and the depletion of striatal dopamine (Blaker and Yamamoto, 2018) after exposure to EtOH + Meth, motor deficits were also attenuated by COX-2 inhibition during EtOH drinking (Fig. 10B). The results indicate that COX-2 activation produced by EtOH drinking further extends the scope and vulnerability of dopamine neurons after Meth to include motor-related dopaminergic deficits in the SNpc similar to that observed in other animal models of Parkinson's disease including Meth exposure to mice (Ares-Santos et al., 2014). Meth alone did not cause significant motor deficits despite a 40% loss of DAT in the striatum (Fig. 7B). This degree of loss is likely not sufficient to cause motor deficits since extrapolations of dopamine depletions to the time of symptom onset do not appear until a 68 to 82% reduction of dopamine in the striatum (Riederer and Wuketich, 1976). Moreover, initial motor deficits in PD only begin to occur when approximately 30% of total SN neurons are lost (Fearnley and Lees, 1991; Greffard et al., 2006). Unlike Meth alone, only the serial exposure to EtOH and Meth resulted in a > 70% loss of DAT immunoreactivity in the striatum and > 40% loss of TH-positive cells in the SNpc and explains why only the combination of EtOH and Meth produced motor deficits measured by performance on the rotarod (Fig. 10B).

5. Conclusions

The present study illustrates an inflammatory response (changes in microglia) in the SNpc after the serial exposure to EtOH and Meth that is associated with a synergistic dopaminergic toxicity (dopamine deficits and motor deficiencies) via apoptosis (cleaved caspase-3) of dopamine cells in the SNpc. The protective effects of nimesulide intervention during EtOH indicates that these effects are mediated by EtOH-induced COX-2, and that events related to induction of COX-2 are involved in the long-term dopaminergic deficits observed after EtOH plus Meth. Furthermore, this damage is unique and distinct from the damage produced by either drug alone, and highlights the role of the inducible inflammatory mediator COX-2 in degeneration of the nigrostriatal pathway.

Acknowledgements

The authors would like to thank Elizabeth Watkins for her assistance with drug administration.

Funding

This work was supported by the National Institutes of Health [DA042737, DA007606].

References

- Anneken, J.H., et al., 2013. MDMA increases glutamate release and reduces parvalbumin-positive GABAergic cells in the dorsal hippocampus of the rat: role of cyclooxygenase. *J. Neuroimmune Pharmacol.* 8, 58–65.
- Ares-Santos, S., et al., 2014. Methamphetamine causes degeneration of dopamine cell bodies and terminals of the nigrostriatal pathway evidenced by silver staining. *Neuropsychopharmacology* 39, 1066–1080.
- Barcia, C., et al., 2012. ROCK/Cdc42-mediated microglial motility and gliapse formation lead to phagocytosis of degenerating dopaminergic neurons in vivo. *Sci. Rep.* 2, 809.
- Barcia, C., et al., 2004. Evidence of active microglia in substantia nigra pars compacta of parkinsonian monkeys 1 year after MPTP exposure. *Glia* 46, 402–409.
- Blaker, A.L., Yamamoto, B.K., 2018. Methamphetamine-induced brain injury and alcohol drinking. *J. Neuroimmune Pharmacol.* 13, 53–63.
- Bujarski, S., et al., 2014. The relationship between methamphetamine and alcohol use in a community sample of methamphetamine users. *Drug Alcohol Depend.* 142, 127–132.
- Carpenter, A.E., et al., 2006. Cell Profiler: image analysis software for identifying and quantifying cell phenotypes. *Genome Biol.* 7, R100.
- Chen, Z., et al., 2012. Lipopolysaccharide-induced microglial activation and neuroprotection against experimental brain injury is independent of hematogenous TLR4. *J. Neurosci.* 32 (34), 11706–11715.
- Cheng, C., Zochodne, D.W., 2003. Sensory neurons with activated caspase-3 survive long-term experimental diabetes. *Diabetes* 52 (9), 2363–2371.
- Crews, F.T., et al., 2007. Systemic LPS causes chronic neuroinflammation and progressive neurodegeneration. *Glia* 55 (5), 453–462.
- Famaey, J.P., 1997. In vitro and in vivo pharmacological evidence of selective cyclooxygenase-2 inhibition by nimesulide: an overview. *Inflammation Res.* 46 (11), 437–446.
- Fearnley, J.M., Lees, A.J., 1991. Ageing and Parkinson's disease: substantia nigra regional selectivity. *Brain* 114 (5), 2283–2301.
- Ferguson, S.A., Cada, A.M., 2004. Spatial learning/memory and social and nonsocial behaviors in the spontaneously hypertensive, Wistar-Kyoto and Sprague-Dawley rat strains. *Pharmacol. Biochem. Behav.* 77, 583–594.
- Greffard, S., Verny, M., Bonnet, A.M., Beinis, J.Y., Gallinari, C., Meaume, S., Piette, F., Hauw, J.J., Duyckaerts, C., 2006. Motor score of the unified parkinson disease rating scale as a good predictor of levty body-associated neuronal loss in the substantia nigra. *Arch. Neurol.* 63 (4), 584–588.
- Hastings, T.G., 1995. Enzymatic oxidation of dopamine: the role of prostaglandin H synthase. *J. Neurochem.* 64 (2), 919–924.
- He, J., Crews, F.T., 2008. Increased MCP-1 and microglia in various regions of the human alcoholic brain. *Exp. Neurol.* 210, 349–358.
- Hernandez-Baltazar, D., et al., 2013. Activation of GSK-3 β and caspase-3 occurs in nigral dopamine neurons during the development of apoptosis activated by a striatal injection of 6-hydroxydopamine. *PLoS One* 8 (8), e70951.
- Hoogland, I.C., et al., 2015. Systemic inflammation and microglial activation: systematic review of animal experiments. *J. Neuroinflamm.* 12, 114.
- Johansson, J.U., et al., 2015. Prostaglandin signaling suppresses beneficial microglial function in Alzheimer's disease models. *J. Clin. Invest.* 125, 350–364.
- Kaushik, D.K., et al., 2013. Interleukin-1 β orchestrates underlying inflammatory responses in microglia via Kruppel-like factor 4. *J. Neurochem.* 127, 233–244.
- Kirkpatrick, M.G., et al., 2012. Acute and residual interactive effects of repeated administrations of oral methamphetamine and alcohol in humans. *Psychopharmacology (Berl)* 219, 191–204.
- Knapp, D.J., Crews, F.T., 1999. Induction of cyclooxygenase-2 in brain during acute and chronic ethanol treatment and ethanol withdrawal. *Alcohol Clin. Exp. Res.* 23 (4), 633–643.
- Koprich, J.B., et al., 2008. Neuroinflammation mediated by IL-1 β increases susceptibility of dopamine neurons to degeneration in an animal model of Parkinson's disease. *J. Neuroinflamm.* 5, 8.
- Kozlowski, C., Weimer, R.M., 2012. An automated method to quantify microglia morphology and application to monitor activation state longitudinally in vivo. *PLoS One* 7, e31814.
- Kuhn, D.M., Francescutti-Verbeem, D.M., Thomas, D.M., 2006. Dopamine quinones activate microglia and induce a neurotoxic gene expression profile. *Ann. N.Y. Acad. Sci.* 1074 (1), 31–41.
- LaVoie, M.J., et al., 2004. Microglial activation precedes dopamine terminal pathology in methamphetamine-induced neurotoxicity. *Exp. Neurol.* 187, 47–57.
- Lawson, L.J., et al., 1990. Heterogeneity in the distribution and morphology of microglia in the normal adult mouse brain. *Neuroscience* 39, 151–170.
- Leslie, E.M., et al., 2017. Simultaneous use of alcohol with methamphetamine but not ecstasy linked with aggression among young adult stimulant users. *Addict Behav.* 70, 27–34.
- Levi, G., et al., 1998. Regulation of prostanoid synthesis in microglial cells and effects of prostaglandin E2 on microglial functions. *Biochimie* 80, 899–904.
- Li, J., et al., 2011. Blockade of GABA(A) receptors in the paraventricular nucleus of the hypothalamus attenuates voluntary ethanol intake and activates the hypothalamic-pituitary-adrenocortical axis. *Addict Biol.* 16, 600–614.
- Loxton, D., Canales, J.J., 2017. Long-term cognitive, emotional and neurogenic alterations induced by alcohol and methamphetamine exposure in adolescent rats. *Prog. Neuropsychopharmacol. Biol. Psychiatry* 74, 1–8.
- Macaya, A., et al., 1994. Apoptosis in substantia nigra following developmental striatal excitotoxic injury. *Proc. Natl. Acad. Sci.* 91 (17), 8117–8121.
- Marinova-Mutafchieva, L., et al., 2009. Relationship between microglial activation and dopaminergic neuronal loss in the substantia nigra: a time course study in a 6-hydroxydopamine model of Parkinson's disease. *J. Neurochem.* 110, 966–975.
- McCann, U.D., et al., 1998. Reduced striatal dopamine transporter density in abstinent methamphetamine and methcathinone users: evidence from positron emission tomography studies with [¹¹C]WIN-35,428. *J. Neurosci.* 18, 8417–8422.
- Naoi, M., Maruyama, W., 1999. Cell death of dopamine neurons in aging and Parkinson's disease. *Mech. Ageing Dev.* 111 (2–3), 175–188.
- Quan, Y., et al., 2013. EP2 receptor signaling pathways regulate classical activation of microglia. *J. Biol. Chem.* 288, 9293–9302.
- Ramesh, T., et al., 2015. Simultaneous quantification of nimesulide, phenylpropranolamine, caffeine and chlorpheniramine in rat plasma by RP–HPLC/PDA method and application to pharmacokinetic studies in healthy rat subjects. *Arab. J. Chem.*
- Rees, K., et al., 2011. Non-steroidal anti-inflammatory drugs as disease-modifying agents for Parkinson's disease: evidence from observational studies. *Cochrane Database Syst. Rev.* CD008454.
- Riederer, P., Wuketich, S., 1976. Time course of nigrostriatal degeneration in parkinson's disease. A detailed study of influential factors in human brain amine analysis. *J. Neural Transm.* 38 (3–4), 277–301.
- Rumpf, J.J., et al., 2017. Structural abnormality of substantia nigra induced by methamphetamine abuse. *Mov. Disord.* 32, 1784–1788.
- Sánchez-Pernaute, R., et al., 2004. Selective COX-2 inhibition prevents progressive dopamine neuron degeneration in a rat model of Parkinson's disease. *J. Neuroinflamm.* 1 (1), 6.
- Sekine, Y., et al., 2008. Methamphetamine causes microglial activation in the brains of human abusers. *J. Neurosci.* 28, 5756–5761.
- Simms, J.A., et al., 2008. Intermittent access to 20% ethanol induces high ethanol consumption in Long-Evans and Wistar rats. *Alcohol Clin. Exp. Res.* 32, 1816–1823.
- Stinson, F.S., et al., 2005. Comorbidity between DSM-IV alcohol and specific drug use disorders in the United States: results from the National Epidemiologic Survey on Alcohol and Related Conditions. *Drug Alcohol Depend.* 80, 105–116.
- Taniguchi, Y., et al., 1997. Inhibition of brain cyclooxygenase-2 activity and the anti-pyretic action of nimesulide. *Eur. J. Pharmacol.* 330, 221–229.
- Tatton, N.A., Kish, S.J., 1997. In situ detection of apoptotic nuclei in the substantia nigra compacta of 1-methyl-4-phenyl-1, 2, 3, 6-tetrahydropyridine-treated mice using terminal deoxynucleotidyl transferase labelling and acridine orange staining. *Neuroscience* 77 (4), 1037–1048.
- Teismann, P., 2012. COX-2 in the neurodegenerative process of Parkinson's disease. *Biofactors* 38, 395–397.
- Teismann, P., Vila, M., Choi, D.K., Tieu, K., Wu, D.C., Jackson-Lewis, V., Przedborski, S., 2003. COX-2 and neurodegeneration in Parkinson's disease. *Ann. N.Y. Acad. Sci.* 991 (1), 272–277.
- Thomas, D.M., Kuhn, D.M., 2005. Cyclooxygenase-2 is an obligatory factor in methamphetamine-induced neurotoxicity. *J. Pharmacol. Exp. Ther.* 313, 870–876.
- Thomas, D.M., et al., 2004. Methamphetamine neurotoxicity in dopamine nerve endings of the striatum is associated with microglial activation. *J. Pharmacol. Exp. Ther.* 311, 1–7.
- Torres-Platas, S.G., et al., 2014. Morphometric characterization of microglial phenotypes in human cerebral cortex. *J. Neuroinflamm.* 11, 12.
- Vijitruth, R., et al., 2006. Cyclooxygenase-2 mediates microglial activation and secondary dopaminergic cell death in the mouse MPTP model of Parkinson's disease. *J. Neuroinflamm.* 3 (1), 6.
- Volkow, N.D., et al., 2001. Loss of dopamine transporters in methamphetamine abusers recovers with protracted abstinence. *J. Neurosci.* 21, 9414–9418.
- Wagner, G.C., et al., 1980. Long-lasting depletions of striatal dopamine and loss of dopamine uptake sites following repeated administration of methamphetamine. *Brain Res.* 181, 151–160.
- Yin, J., Valin, K.L., Dixon, M.L., Leavenworth, J.W., 2017. The role of microglia and macrophages in CNS homeostasis, autoimmunity, and cancer. *J. Immunol. Res.*